Available online at www.sciencedirect.com
ScienceDirect
Scripta Materialia 60 (2009) 236–239
Scripta MATERIALIA
www.elsevier.com/locate/scriptamat

Grain boundary sliding during friction stir spot welding of an aluminum alloy

A.P. Gerlich[a,*] and T. Shibayanagi[b]

[a] University of Alberta, Chemical and Materials Engineering, 536 CME Building, Edmonton, AB, Canada T6G 2G6
[b] Osaka University, Joining and Welding Research Institute, Osaka 567–0047, Japan

Received 26 August 2008; revised 8 October 2008; accepted 9 October 2008
Available online 17 October 2008

The grain and dislocation structures in an Al–4.3Cu–1.4Mg alloy friction stir spot weld made using tool rotational speeds from 750 to 1500 rpm are investigated. The stir zone region contains grains with random boundaries, where grains with dimensions <250 nm are free of dislocations, and grains having average dimensions >500 nm possessed high dislocation densities. Dislocation annihilation is negligible during the spot welding process. Grain boundary sliding accounts for the low dislocation density in grains having sizes <250 nm.

Keywords: Friction stir; Spot welding; Grain boundary sliding; Al 2024

The friction stir welding process was developed by TWI, Abington, UK in 1991 for joining aluminum alloys [1]. The two overlapping sheets are joined at a single location during friction stir spot welding and the rotating tool is withdrawn leaving a keyhole depression. The stir zone region comprises dynamically recrystallized material formed adjacent to the rotating tool in a cycle time typically ranging from 1 to 5 s [2]. The microstructure of the stir zone region comprises a fine-grained microstructure with predominantly high-angle grain boundaries [2,3].

Although it has been generally assumed that grain boundary sliding occurs during friction stir welding [4], no microstructural evidence has been provided. Gerlich et al. [2,5,6] estimated the strain rate at the contact interface during friction stir spot welding by incorporating measured stir zone temperature and average grain size values into the Zener–Hollomon relation. Metallographic evidence confirming local melting has been found in Al 7075-T6 and Al 2024-T3 spot welds produced using rotational speeds of 3000 rpm, and was associated with spontaneous melting of second-phase particles [7]. It was suggested that melting promoted grain boundary sliding in the stir zone of the friction stir spot weld [6], since it is observed that grain boundary sliding during high-temperature deformation is enhanced by the presence of liquid films [8–11]. Grain boundary sliding will favor texture randomization [12] and this feature has already been observed in the stir zones of Al 2024 spot welds [6]. Since these findings were observed in spot welds containing liquid films, the question remains whether evidence of grain boundary sliding can be found in friction stir spot welds where there is no metallographic evidence of local melting.

The present paper examines grain boundary sliding during friction stir spot welding of Al 2024 base material using tool rotation speeds from 750 to 1500 rpm when the spot welding temperature remains below the melting temperature of Al_2CuMg second-phase particles (763 K) [13] and no melted films are observed in the stir zone. Grain and dislocation structures are examined, as well as the grain boundary misorientation distributions produced in the location immediately adjacent to the pin periphery.

Electron backscattered diffraction (EBSD) microscopy is used to determine the average subgrain dimensions in the stir zones of Al 2024 spot welds made using different tool rotational speed settings. Transmission electron microscopy (TEM) is used for the detailed examination of the dislocation structures. The chemical composition of the 6.3 mm thick Al 2024 base material employed was 4.30% Cu, 1.42% Mg 0.15% Fe, 0.62% Mn, 0.07% Si, 0.03% Ti, 0.07% Zn and <0.01% Cr (all wt.%). The tool geometry comprised a 10 mm diameter

* Corresponding author. Tel.: +1 780 492 8853; fax: +1 780 492 2881; e-mail: gerlich@ualberta.ca

1359-6462/$ - see front matter
doi:10.1016/j.scriptamat.2008.10.006

shoulder, a pin diameter of 4 mm and a pin length of 2.2 mm. A detailed description of the spot welding equipment and temperature measurement set-up is provided elsewhere [14]. The stir zone temperature is determined by locating a thermocouple within the tool itself, at the side of the pin and 0.2 mm from the tip of the tool. All temperature measurements were repeated at least three times at each welding parameter setting.

A location adjacent to the tool pin at a distance of 0.1 mm from the keyhole (and midway down the length of the pin) was examined in friction stir spot welds using both EBSD and TEM. EBSD was carried out using a Hitachi S-4500 field emission scanning electron microscope with TSL TexSEM software using a step size of 0.2 μm. The surface of the sample was mechanically polished and electropolished using a solution of 25 vol.% of HNO_3 and 75 vol.% of methanol at a temperature of −30 °C and a voltage of 12 V. TEM samples were prepared from 3 mm disks removed from the stir zone using a low-speed diamond saw were thinned with a twinjet electropolisher, using identical conditions to those employed during EBSD electropolishing. During TEM, the test samples were examined using a JEOL 2010 microscope operating at 200 kV.

The stir zone material experiences drastic heating rates averaging from 212 to 385 K s^{-1} during the tool penetration phase (in the first 1.3 s) when friction stir spot welding Al 2024-T3 alloy [6]. Following tool penetration, tool rotation continued for 4 s with the shoulder in contact with the Al alloy plate, during which the temperature gradually increased to the peak. The highest average temperature values measured at the location 0.2 mm from the tip of the rotating pin increased from 707 to 770 K when the tool rotational speed increased from 750 to 3000 rpm (see Table 1).

Figure 1 shows the EBSD misorientation map in a spot weld made using a tool rotational speed of 1125 rpm. The direction of the shear stress imposed on the stir zone during tool rotation is indicated by the arrows. Subgrain boundaries (having misorientations from 2° to 15°) are shown using thin lines, while grain boundaries (having misorientations >15°) are shown using thick lines. The average grain sizes calculated from EBSD data are summarized in Table 1 for each tool rotation speed examined. The fraction of high-angle grain boundaries varied from 67.5% to 95.9%, and the misorientation distributions for spot welds made using tool rotational speeds from 750 to 1125 rpm are shown in Figure 2. There was a random distribution of high-angle boundaries and the proportion of low-angle boundaries was higher when the tool rotation speed increased to 1125 rpm.

Table 1. Peak pin temperatures and stir zone grain sizes.

Tool (rpm)	Pin temperature (K)	d_{avg} (μm)[a]
750	683 ± 27.2	0.57 ± 0.03
950	707 ± 16.6	1.02 ± 0.16
1125	712 ± 9.0	0.40 ± 0.06
1500	750 ± 2.4	0.80 ± 0.06
2250	765 ± 1.0	0.87 ± 0.09
3000	770 ± 7.2	1.27 ± 0.16

[a] The error ranges correspond to one standard deviation above and below the mean value.

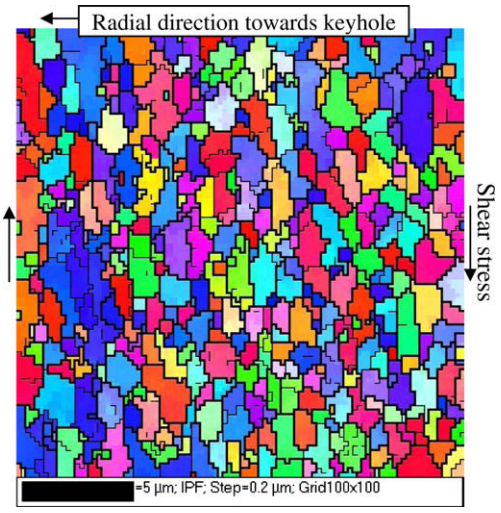

Figure 1. EBSD misorientation map showing subgrain boundaries (thin lines) and grain boundaries (thick lines) in the stir zone of an Al 2024 spot weld produced using a tool rotational speed of 1125 rpm. EBSD data was collected in the rolling plane of the base material. The orientation of shear stress during welding is indicated by the arrows.

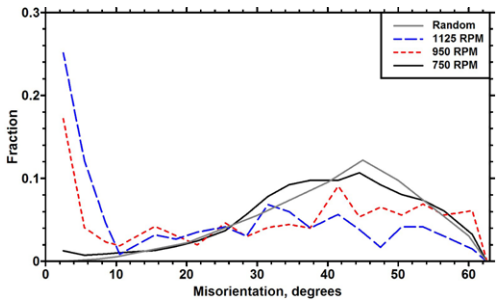

Figure 2. EBSD misorientation statistics for spot welds made using tool rotational speeds of 750, 950 and 1125 rpm.

Grain boundary sliding is recognized as the primary mechanism during superplastic deformation of fine-grained materials [15]. A fine-grained equiaxed microstructure in conjunction with a large fraction of high-angle boundaries promotes grain boundary sliding [16,17], and grains slightly elongate in the direction of applied stress during superplastic deformation [18]. These features are readily apparent in Figures 1 and 2. In this connection, high strain rate superplasticity has been demonstrated in friction stir processed Al 2024 material when it is loaded in tension at temperatures ranging from 703 to 723 K. In this case, the Al 2024 material had a microstructure comprising equiaxed grains containing >95% high-angle grain boundaries [19]. During grain boundary sliding the net contribution to external strain resulting from dislocation movement is nearly zero [20].

The average grain sizes found using EBSD were similar to those found using TEM, with at least 170–450 grains examined using both techniques for each tool rotation speed. More than 120 grains were observed using TEM which seldom contained dislocations and

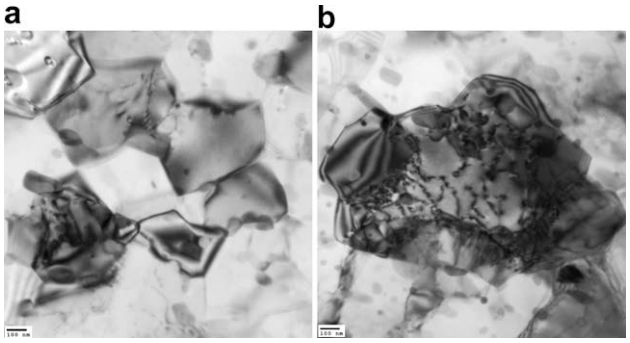

Figure 3. TEM micrographs of the stir zone in an Al 2024 spot weld made using a tool rotational speed of 1125 rpm.

had dimensions <250 nm (see Fig. 3a). In contrast, grains having dimensions >500 nm had high dislocation densities (see Fig. 3b). This trend was also observed in friction stir spot welds made using tool rotation speeds of 750 and 950 rpm (see Fig. 4). Similar microstructural observations were reported when examining the superplastic deformation behavior of friction stir processed Al 7075 base material [21,22]. In Al 7075, small grains having dimensions from 100 to 250 nm were free of dislocations, while grains having dimensions from 200 to 400 nm contained randomly distributed dislocations [23].

Figures 3 and 4 also indicate that grains <250 nm in diameter exhibit thick grain boundary extinction contours, indicating the presence of a high level of internal stresses in the vicinity of the grain boundaries [24]. The appearance of such contours is commonly observed in materials exhibiting superplasticity via grain boundary sliding [18].

Since grains with diameters <250 nm in the stir zone have a very low dislocation density, their deformation behavior following their formation will be primarily determined by grain boundary sliding and not by dislocation glide. During superplastic deformation, an intragranular strain ε'_{IS} due to accumulated dislocations is needed to accommodate the rearrangement of adjacent grains during sliding. The intragranular strain in an individual grain can be estimated by $\varepsilon'_{IS} = \rho bL$, where ρ is the density of dislocations absorbed by the grain boundaries during superplastic deformation, b is the Burger's vector (0.286 nm) and L is the distance traveled by each dislocation, being approximately equal to the grain size [25]. It is apparent that when the grain size decreases, the amount of intragranular strain accommodated by each grain will decrease and the likelihood of observing dislocations within a grain will diminish.

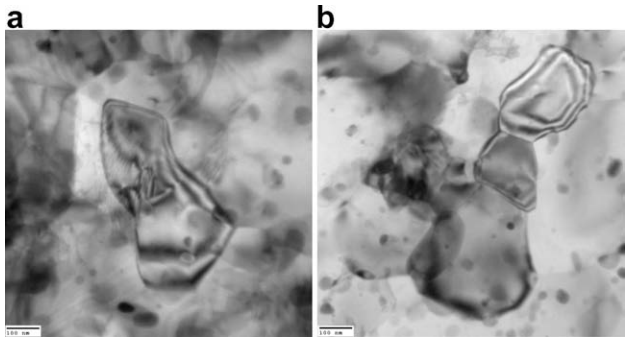

Figure 4. TEM micrographs of the stir zone in Al 2024 spot welds made using tool rotational speeds of (a) 750 rpm, and (b) 950 rpm.

The low dislocation densities observed in grains having dimensions <250 nm may be caused by dislocation annihilation at the grain boundaries following dislocation climb. In order to determine if dislocation climb in the stir zone at high temperature can account for the dislocation-free grain structures in grains with diameters <250 nm, it is necessary to calculate the image force on a dislocation and the corresponding velocity during dislocation climb. For example, the climb of dislocations towards a grain boundary is determined by the image force F:

$$F = -\frac{\mu b^2}{4\pi l}, \tag{1}$$

where μ is the shear modulus of the material (28 GPa [26]), and l is the distance from the grain boundary (assumed to be 125 nm, the radius of small dislocation-free grains) [27]. The image force for a dislocation located at the center of a 250 nm diameter grain in Al 2024 is 1.46×10^{-3} N m^{-1} and the dislocation velocity (v_d) is:

$$v_d = D_s c_j \frac{Fb}{kT}, \tag{2}$$

where D_s is the constant for self-diffusion (3.96×10^{-14} m^2 s^{-1} at 775 K [28]), k is the Boltzmann's constant and T is the temperature in degrees Kelvin. The average density of dislocation jogs (c_j) is determined by the following relation [27]:

$$c_j \approx \exp\frac{-U_j}{kT}, \tag{3}$$

where U_j is the energy of formation of a jog approximated by $0.1\mu b_1^2 b_2$, and b_1, b_2 are both 0.286 nm [27]. Using these values, c_j and v_d are 2.19×10^{-3} m^{-2} and 3.4×10^{-9} m s^{-1}, using the reported solidus temperature of Al 2024 (775 K) as an upper limit. Based on these calculations, dislocations contained in small 250 nm diameter grains are not able to climb a significant distance during the short cooling period (several seconds) following completion of the friction stir spot welding operation. Also, since the stir zone temperature is less than 775 K during the dwell period in friction stir spot welding, the average distance that dislocations can diffuse in a dwell time of 4 s is <14 nm. Since these calculations neglect dislocation interaction, the actual velocity may be even slower if dislocation entanglement occurs.

It is well established that during high-temperature creep, the grain size, d, is related to the applied stress, τ, through the following relationship:

$$\frac{d}{b} = \zeta\left(\frac{\tau}{\mu}\right)^{-1}, \tag{4}$$

where ζ is a constant approximately equal to 10 [29]. The strain rates produced during friction stir spot welding are much higher than those examined during creep testing, however the relation in Eq. (4) may be used to approximate the upper limit for grain size during grain

boundary sliding and superplasticity since it is independent of the strain rate. Since the applied stress in the stir zone cannot be directly determined from the experimental data, Colegrove and Shercliff [30,31] used numerical modeling to determine that the von Mises equivalent flow stress produced close to the periphery of the rotating tool during Al 2024 friction stir welding is approximately 40 MPa when a tool rotational speed of 1600 rpm is applied [32]. This value is comparable to the tensile stress observed during mechanical testing of Al 2024 at 407 °C [26]. Based on this stress value and Eq. (4), one would expect that grain boundary sliding and superplasticity in Al 2024 would occur during friction stir spot welding providing the grain size is less than 2 μm.

It should be noted that grain boundary sliding does not necessarily occur in all grains within the stir zone, since they have nearly random orientations as shown in Figures 1 and 2, and hence the Schmidt factors will not favor grain boundary sliding in all grains. However, it is argued that grain boundary sliding would be particularly likely to occur in grains with sizes <250 nm, since it has already been shown that grain boundary sliding becomes a dominant deformation mode as grain size decreases [15]. These results provide support for the proposal that grain boundary sliding occurs in Al 2024 friction stir spot welds made at rotational speeds of 750–1125 rpm.

In conclusion, the dislocation structures found in Al 2024 friction stir spot welds produced at 750–1500 rpm have been examined. TEM observation revealed that grains having diameters <250 nm are free of dislocations, while grains having diameters >500 nm contain dislocation densities, which are typical of a deformed microstructure. It is suggested that grain boundary sliding during the Al 2024 friction stir spot welding accounts for the low dislocation densities observed in the small diameter grains. The intragranular strain during grain boundary sliding decreases with decreasing grain size and accounts for the low frequency of dislocations contained in grains having diameters <250 nm. In addition, dislocation annihilation in the vicinity of grain boundaries will not play a significant role in reducing the dislocation density, since the dislocation climb rate is negligible.

The authors acknowledge the financial support from the Natural Sciences and Engineering Research Council of Canada during this project. Discussions with Prof. T. Langdon are also greatly appreciated.

[1] W.M. Thomas, E.D. Nicholas, J.D. Needham, M.G. Murch, P. Temple-Smith, C.J. Dawes, GB Patent Application No. 9125978.8, Dec. 1991; US Patent No. 5460317, Oct. 1995.
[2] A. Gerlich, G. Avramovic-Cingara, T.H. North, Met. Trans. A. 37A (2006) 2773.
[3] A. Gerlich, P. Su, T.H. North, J. Mater. Sci. 40 (2005) 6473.
[4] R. Nandan, T. DebRoy, H.K.D.H. Bhadeshia, Prog. Mat. Sci. 10.1016/j.pmatsci.2008.05.001.
[5] A.P. Gerlich, Doctoral Thesis, University of Toronto, Toronto, Canada, 2007.
[6] A. Gerlich, P. Su, M. Yamamoto, T.H. North, J. Mater. Sci. (2007), doi:10.1007/s10853-006-1103-7.
[7] H.J. McQueen, J.E. Hockett, Met. Trans. 1A (1970) 2997.
[8] T.G. Nieh, J. Wadsworth, T. Imai, Scripta Metall. Mater. 26 (1992) 703.
[9] M. Mabuchi, K. Higashi, T.G. Langdon, Acta Metall. Mater. 42 (1994) 1739.
[10] M. Mabuchi, K. Higashi, Mater. Sci. Eng. A179/A180 (1994) 625.
[11] K. Higashi, T.G. Nieh, M. Mabuchi, J. Wadsworth, Scripta Metall. Mater. 32 (1995) 1079.
[12] M.T. Pérez-Prado, G. González-Doncel, O.A. Ruano, T.R. McNelley, Acta Mater. 49 (2001) 2259.
[13] X.-M. Li, M.J. Starink, Mater. Sci. Technol. 17 (2001) 1324.
[14] A. Gerlich, M. Yamamoto, T.H. North, J. Mater. Sci. (2008), doi:10.1007/s10853-007-1791-7.
[15] A.V. Sergueeva, N.A. Mara, N.A. Krasilnikov, R.Z. Valiev, A.K. Mukherjee, Phil. Magn. 86 (2006) 5797.
[16] Y. Xun, M.J. Tan, T.G. Nieh, Mater. Sci. Tech. 20 (2004) 173.
[17] T.G. Nieh, J. Wadsworth, O.D. Sherby, Mater. Sci. Forum 243–245 (1997) 11.
[18] O.A. Kaibyshev, F.Z. Utyashev, Superplasticity: Microstructural Refinement and Superplastic Roll Forming, Futurepast, Arlington, 2005.
[19] I. Charit, R.S. Mishra, Mater. Eng. A359 (2003) 290.
[20] R.Z. Valiev, T.G. Langdon, Acta Metall. 41 (1993) 949.
[21] R.S. Mishra, M.W. Mahoney, S.X. McFadden, N.A. Mara, A.K. Mukherjee, Scripta Mater. 42 (2000) 163.
[22] Z.Y. Ma, R.S. Mishra, M.W. Mahoney, Acta Mater. 50 (2002) 4419.
[23] J.-Q. Su, T.W. Nelson, C.J. Sterling, Scripta Mater. 52 (2005) 135.
[24] O.A. Kaibyshev, Scientific Bases, Achievements and Promises of Superplastic Deformation, Gilem, Ufa, Russia, 2000.
[25] R.Z. Valiev, T.G. Langdon, Acta Metall. Mater. 41 (1993) 949.
[26] J.G. Kaufman, Properties of Aluminum Alloys, ASM International, Materials Park, OH, 1990.
[27] J. Friedel, Dislocations, Pergamon Press, Oxford, 1964.
[28] S.L. Robinson, O.D. Sherby, Phys. Stat. Sol. A (1970) K119.
[29] T.G. Langdon, Z. Metallkd. 96 (2005) 522.
[30] P.A. Colegrove, H.R. Shercliff, Sci. Technol. Weld. Join. 9 (2004) 483.
[31] P.A. Colegrove, H.R. Shercliff, Sci. Technol. Weld. Join. 11 (2006) 429.
[32] P.A. Colegrove, H.R. Shercliff, R. Zettler, Sci. Technol. Weld. Join. 12 (2007) 284.